

## Regular article

# A novel structure of YSZ coatings by atmospheric laminar plasma spraying technology

Sen-Hui Liu<sup>a</sup>, Cheng-Xin Li<sup>a,\*</sup>, Hui-Yu Zhang<sup>a</sup>, Shan-Lin Zhang<sup>a</sup>, Lu Li<sup>b</sup>, Pan Xu<sup>b</sup>, Guan-Jun Yang<sup>a</sup>, Chang-Jiu Li<sup>a</sup>

<sup>a</sup> State Key Laboratory for Mechanical Behavior of Materials, School of Materials Science and Engineering, Xi'an Jiaotong University, Xi'an, Shaanxi 710049, China

<sup>b</sup> Zhenhuo Plasma Technology Company, Chengdu, Sichuan 610065, China



## ARTICLE INFO

## Article history:

Received 6 January 2018

Received in revised form 9 April 2018

Accepted 13 April 2018

Available online xxx

## Keywords:

Laminar plasma jet

YSZ coatings

Thermal conductivity

Particles velocity

Vapor deposition

## ABSTRACT

A novel structure of yttria stabilized zirconia coatings was developed in this study by a newly laminar plasma spraying technology in atmospheric environment. The unique microstructures of coatings showed the multi-island protrusions feature at the top surface, quasi-columnar structures along the cross-section distributed as a certain interval and hybrid droplet/vapor deposited structures at the fracture surface. The distributions of particle velocity and surface temperature along the axial direction of long laminar plasma jet were investigated and compared with other plasma spraying methods. The effects of different microstructures to thermal conductivities comparing with other current plasma spray methods were also demonstrated.

© 2018 Acta Materialia Inc. Published by Elsevier Ltd. All rights reserved.

Plasma sprayed thermal barrier coatings (TBC) of low-thermal conductivity have been extensively used to provide thermal insulation for metallic components in gas turbine engines [1–3]. A typical thermal barrier coating system on the surface of superalloy substrate consists of an oxidation-resistant metallic bond coating and a ceramic top coating [4,5]. Yttria stabilized zirconia (YSZ) of low thermal conductivity, high toughness and melt temperature has been widely used as the top coatings materials [2]. The YSZ top coating is deposited by either electron-beam physical-vapor deposition (EB-PVD) method [6] or plasma-spray deposition (APS, SPS, PS-PVD) methods [7,10]. The EB-PVD coating with columnar microstructures performed high thermal cyclic life-time and also high thermal conductivity (usually  $1.5\text{--}2.0\text{ W m}^{-1}\text{ K}^{-1}$ ) [8,9]. The typically atmospheric plasma sprayed YSZ coatings with lamellar structure possessed low adhesive strength and low thermal conductivity (usually  $0.8\text{--}1.8\text{ W m}^{-1}\text{ K}^{-1}$ ) [10,11,32].

Technically, current plasma spray methods (APS, SPS and PS-PVD) are using the direct current non-transferred arc plasma torch with linear channel structures for thermal spray process, like the commercial Sulzer serials 9 M torches, Sulzer F4VB torch, Sulzer Triplex serials torches or Praxair serials SG-100 Guns. The arc is operated across a flow of argon,

hydrogen, helium, nitrogen or mixtures between a cathode (Sulzer Triplex serials torches with three cathodes [12]) and a nozzle-shaped water-cooled anode where the plasma gas is induced along the cylindrical channel and injected into the surrounding environment [13]. The lengths of these plasma jets that generated by the conventional non-transferred arc plasma torches cannot exceed 200 mm in atmospheric environment at a minimum gas flow rate of 30 slpm [10], the spraying distance in atmospheric environment usually is in the range of 80 mm–200 mm [14]. Except for the PS-PVD process, it can obtain an expansion flow of plasma jet in a length from 1000 mm to 2000 mm and a diameter from 200 mm to 400 mm only when the plasma torch is in a closed-chamber at a low-pressure condition [15].

In atmospheric plasma spraying YSZ coating process, the working power and total gas flow rate for atmospheric plasma spraying YSZ coatings usually exceed 30 kW and 40 slpm, respectively [4,5,16]. The ceramic powders that suspended in carrier gas are injected into the thermal plasma plume in radial or axial direction, where solid powders are accelerated and heated to molten or semi-molten state. Finally, these particles continuously impinge on the prepared substrate to form coatings of numerous overlapped splats. The microstructure of coatings features the lamellar structure consisted of overlapped splats and this process cannot obtain abundant vapor-deposited coatings in atmospheric environment.

In addition, for the PS-PVD process, these systems usually work at input power ranging from 65 kW to 150 kW and total gas flow rate ranging from 80 slpm to 200 slpm [7,15,19,21]. At these conditions, the injected YSZ powder can be vaporized sufficiently and obtained

*Abbreviations:* APS, atmospheric plasma spray; ALPS, atmospheric laminar plasma spray; EB-PVD, electron-beam physical-vapor deposition; PS-PVD, plasma sprayed-physical vapor deposition; SEM, scanning electron microscopy; SPS, suspension plasma spray; TBC, thermal barrier coating; YSZ, yttria stabilized zirconia.

\* Corresponding author.

E-mail address: [licx@mail.xjtu.edu.cn](mailto:licx@mail.xjtu.edu.cn) (C.-X. Li).

**Table 1**  
Laminar plasma spraying parameters.

Parameters	Value
Input power/ kW	25–26
Torch move velocity/ m/s	0.6
Torch move interval/ mm	4
Spraying distance/ mm	250
Plasma gas N <sub>2</sub> /Ar	7:3 (by volume)
Total gas flow rate/ slpm	14
Feed powder	YSZ (Metco6700)
Powder feed rate/ g/min	4 (no carrier gas)

lamellar, hybrid, quasi-columnar, EB-PVD-liked columnar type or column type YSZ coatings in different spraying distances. The results show low thermal conductivity (usually  $0.5\text{--}1.2\text{ W m}^{-1}\text{ K}^{-1}$ ) and excellent thermal cycling performances than the conventional atmospheric plasma spray method (APS) [17–19]. It also provides a method in higher deposition rate and lower investment costs than EB-PVD process [20,21].

Therefore, a mass of vapor deposited YSZ coatings can only be obtained under the low-pressure conditions, liked PS-PVD or EB-PVD process. Conventional atmospheric plasma spray technology cannot obtain abundant vapor-deposited YSZ coatings that consisted of column-type or quasi-column features.

In this work, a novel long laminar plasma jet that generated by a newly type of non-transferred arc plasma torch was used in atmospheric thermal spray process. The lengths of plasma jet can be changed range from 200 mm to 700 mm in atmospheric environment at different working conditions [22]. This method can also obtain quasi-columnar structure YSZ coatings with abundant vapor-phases at the input power of 25–26 kW ( $I = 160\text{ A}$ ) and total gas flow rate of 14 slpm by 70% nitrogen and 30% argon in atmospheric condition.

7%–8% yttria stabilized zirconia spheroidal powder (Metco 6700,  $-30\text{ }\mu\text{m} \sim +1\text{ }\mu\text{m}$ ,  $d_{50} = 10\text{ }\mu\text{m}$ , Oerlikon Metco, Westbury, USA) was used as the feedstock material, which was a fine and agglomerated powder specifically designed for Plasma Sprayed Physical Vapor Deposition (PS-PVD) coating process [23]. The particles injection in this work was through a specific gravity-vibration device in the radial direction of torch nozzle and did not use the conventional powder supply by the way of auxiliary gas [24]. The initial injecting velocity was less than 3 m/s at the mass flow rate of 4 g/min. The substrate used in coating deposition was 304 stainless steel, which was prepared after grit-blasting, with a NiCoCrAlY bond coating having a thickness of 40  $\mu\text{m}$  deposited by a low-pressure plasma spraying (LPPS) system (Ni23Co20Cr8.5Al4.0Ta0.6Y, Amdry 997,  $-37\text{ }\mu\text{m} \sim +9\text{ }\mu\text{m}$ , Sulzer Metco, Westbury, NY) [25]. The details of laminar plasma spray process were shown in Table 1.

The thermal conductivity is calculated by Eq. (1):

$$\lambda = \alpha \cdot C_p \cdot \rho \quad (1)$$

where  $\alpha$  is the thermal diffusivity in  $\text{m}^2/\text{s}$ ,  $C_p$  is the specific heat capacity in  $\text{J}/(\text{kg K})$ ,  $\rho$  is the density in  $\text{kg}/\text{m}^3$ , and  $\lambda$  is the thermal conductivity in  $\text{W}/(\text{m K})$  [26]. The thermal diffusivities ( $\alpha$ ) of the YSZ coatings were measured using a laser-flash apparatus (Netzsch, LFA-427, Germany).

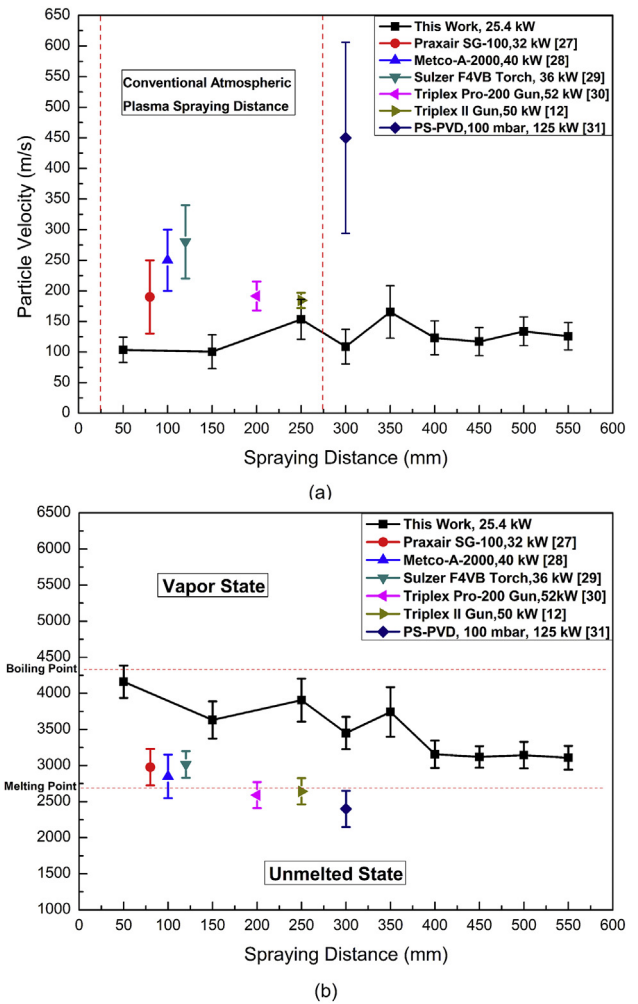


**Fig. 2.** Particle velocity (a) and particle surface temperature (b) in laminar plasma jet at different positions from the nozzle exit and comparison with the results from other plasma spray methods.

The diameter of the specimens was designed as 12.7 mm–13 mm. The surfaces of the specimens were coated with a thin film of graphite for thermal absorption of laser pulses at the beginning. Each sample was measured three times at one selected temperature. The value of the heat capacity of the coatings was determined with differential scanning calorimeters (Netzsch-404, Germany).

As Fig. 1-a showed the photo of long laminar plasma jet in atmospheric environment. The YSZ powders that injected at the radial direction of nozzle exit were accelerating and heating in laminar plasma jet (Fig. 1-b). The in-situ experimental measurement results of particle velocity and surface temperature as a function of spraying distances were plotted in Fig. 2-a and Fig. 2-b, respectively. Moreover, other results in Fig. 2 were from the APS methods by five typically commercial plasma torches [12,27–30], which used spherical hollow 7–8% YSZ particles as



**Fig. 1.** Photos of the laminar plasma jet in atmospheric air (a) and with YSZ particles heating and accelerating of (b).

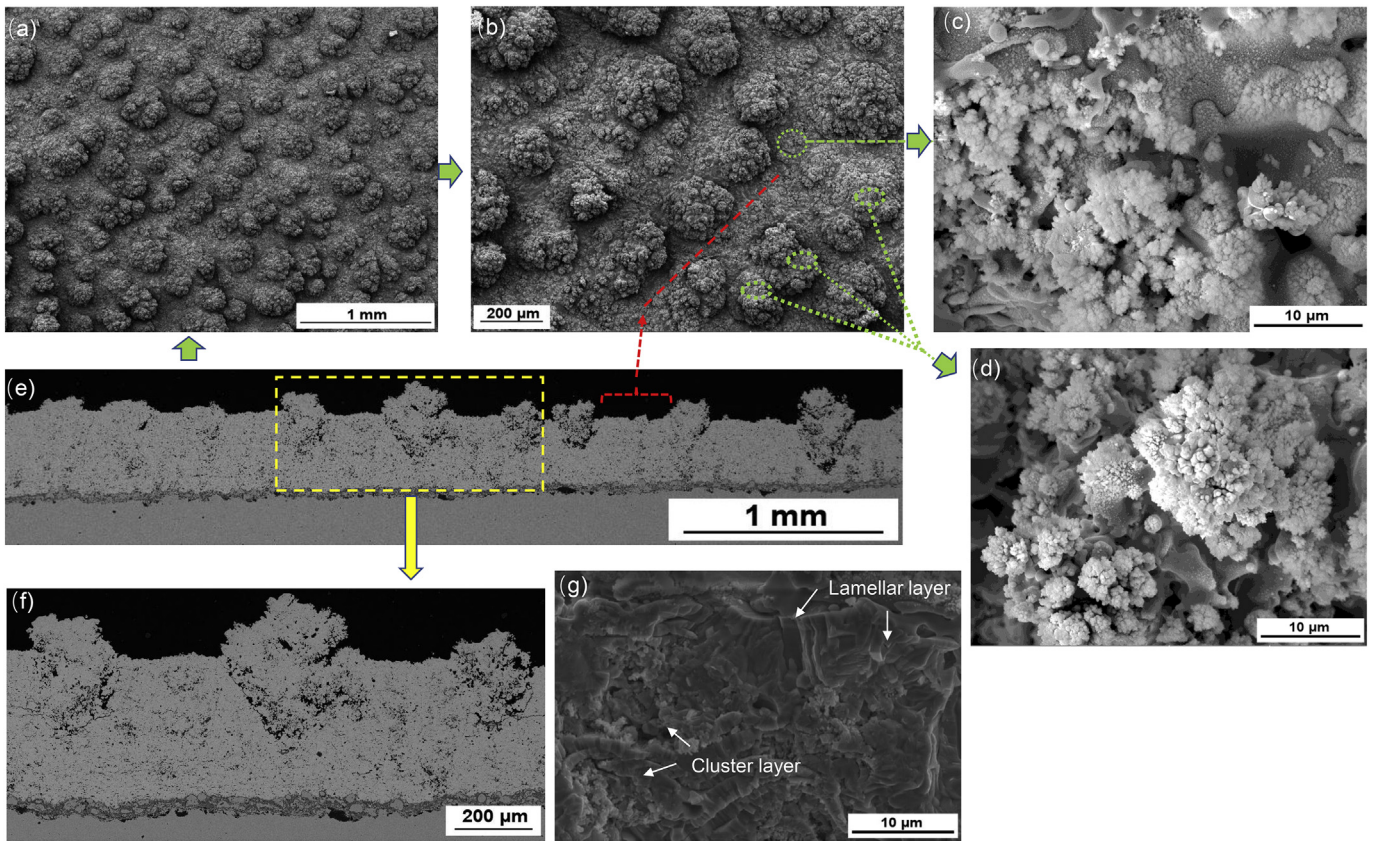


Fig. 3. Top surfaces (a, b, c, d), polished cross sections (e, f) and fracture surface (g) of YSZ coating at the spraying distance of 250 mm.

the feed materials. The results in PS-PVD process was also shown in Fig. 2 that using the same powders as this work (Metco 6700,  $-30 \mu\text{m} \sim +1 \mu\text{m}$ ,  $d_{50} = 10 \mu\text{m}$ , Oerlikon Metco, Westbury, USA) [31]. These results in Fig. 2 all measured by the Technar DVP-2000 particle optical sensor system (Technar Automation Ltd., Canada), which is the widely used commercial particle analysis device in spray research areas [32]. The sensor of DPV-2000 particle diagnostics system had an XY positioning unit which allowed a cross section of this laminar plasma jet to be scanned perpendicularly to the spray axis.

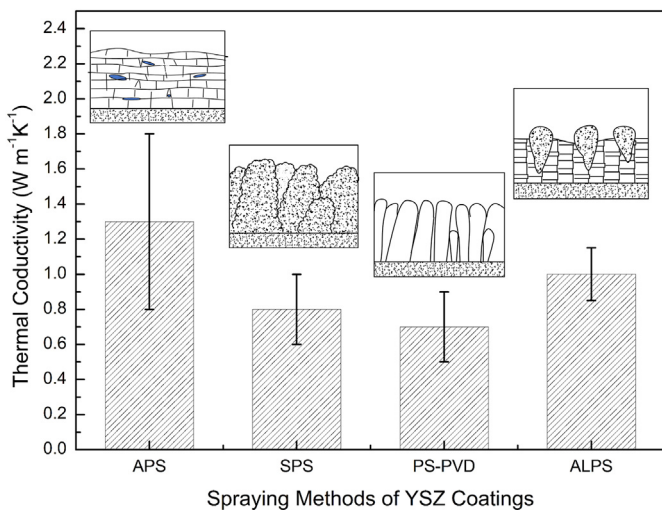


Fig. 4. Thermal conductivities at the room temperature of the YSZ coatings from four plasma spraying technologies.

Comparing with other plasma spray methods, the injected particles went through a long accelerating and heating distance when flowing into this laminar plasma plume. The particles can be accelerated to the mean velocity level of 100 m/s  $\sim$  170 m/s at the distance ranging from 50 mm  $\sim$  550 mm from the nozzle exit. The distributions of particle surface temperature were almost higher than the melting point temperature of YSZ. The mean particle velocity of other methods at different spraying distances were all greater than this work (Fig. 2-a), although the results of particle surface temperature at different positions were all lower than this work (Fig. 2-b). In conventional atmospheric plasma spraying processes in Fig. 2, the velocity and the temperature of the particles were two of the most important parameters influencing the coating microstructure. The particle heating distance and dwell time were all shorter than this work; In PS-PVD process of Fig. 2, the particle velocity and temperature were influenced by both the plasma plume and the low-pressure condition, which can obtain an extremely high particle velocity.

Fig. 3 showed the comprehensive microstructure views of YSZ coatings at the spraying distance of 250 mm using this laminar plasma spray system in ambient air. The microstructure morphologies of YSZ coatings were characterized by a scanning electron microscope (SEM, VEGA II, TESCAN, Czech). Keyence color 3D laser scanning microscope (VK-9700, violet laser) was operated to measure the top surface roughness of the coatings. Observations included top surfaces (Fig. 3-a, b, c, d), polished cross-section surfaces (Fig. 3-e, f) and the fracture surface (Fig. 3-g). The minimum thickness of the coatings was over than 200  $\mu\text{m}$ .

The top surface of the coating was characterized by multi-island protrusions of the mean roughness of 39.8  $\mu\text{m}$  (Ra), which was larger than the maximum size of original YSZ powders. The tops of every island-protrusions consisted of the aggregation of vapor deposited cluster-linked structures and without clearly unmelted particles from the lower

and higher magnification views of the top surface SEM images (Fig. 3-b, d). A mass of vapor deposited cluster structures can also be found at the interspace of every two protrusions (Fig. 3-c). The interspace between two island protrusions just corresponded to the flat region from the polished cross-section observations in Fig. 3-e.

The polished cross section of coating presented a net-like feature of voids and porous-layer (Fig. 3-e, f); the top surface island-protrusions embedded into the previously solidified layers and distributed along the transverse direction as a certain interval. The micro sizes of voids and pores on the cross sections were much smaller than the height of top protrusions. The fracture section showed a mixture of typical lamellar layers composed of numerous solidified splats and micro-sized cluster layers (Fig. 3-g). The thickness of each lamellar layer was about 2  $\mu\text{m}$ . Therefore, the multi-island protrusions at the top surface were consisted of fully vapor-deposited YSZ powders, which showed a quasi-column microstructure at the cross-section. The interspace of multi-island protrusions was consisted of hybrid vapor and droplet phases.

As the laminar plasma jet that carried powders produced a very focused deposition spot onto the surface of substrates, the deposition rate in this work was about 4000  $\mu\text{m}/\text{h}$  at the torch moving speed of 0.6 m/s and intervals of 4 mm. Using this atmospheric laminar plasma spray technology can also obtain a mass of co-deposition of droplet and vapor YSZ particles at atmospheric environment under lower input power than other methods. This may provide a new option for different plasma spraying applications and improve the controllability of plasma spraying technology.

Thermal conductivity is the most important thermo-physical material parameter for characterizing the thermal transport properties of YSZ coatings. Fig. 4 presented the thermal conductivities of YSZ coatings by this work and compared with results from other typical plasma spray methods. There represented four kinds of typical microstructures of YSZ coatings by current plasma spray methods. The differences in thermal conductivities of the four results were mostly influenced by the microstructures and pore size distributions. The pores, voids and cracks networks in lamellar structures that can enhance the phonon scattering and reduce the phonon mean free path were recognized as vital factors in reducing the thermal conductivity [19]; microstructural features like less columnar density, small inter-columnar spaces and more abundant grain boundaries from numerous nano/micro-nano pores of columnar types in SPS coatings can lead to more low thermal conductivity [18,33]; The PS-PVD process produced the column type consist of a high amount of internal porosity, which increases the number of grain boundaries and also lead for low thermal conductivity of YSZ coatings [20,21]. In this work, the microstructural frameworks constituted of randomly oriented micro-voids, isolated interlamellar pores and quasi-columnar microstructure all attributed to the low thermal isolation property of coatings. Hence, it is important to control these kinds of features within coatings in order to control the overall thermal properties of the TBCs.

To summarize, the above results and discussions presented a novel structure YSZ coating by long laminar plasma spraying technology at the conditions of input power of 25–26 kW, gas flow rate of 14 slpm by 70% nitrogen and 30% argon in atmospheric environment. The

refractory 8YSZ powder can be melted efficiently in long laminar plasma jet and obtained co-deposition structure with droplet and vapor phases eventually. This unique hybrid microstructures of coatings exhibit a new option of thermal barrier coatings and this new method improved the working environment of workers and the controllability of the atmospheric plasma spraying technology.

This work was supported by the Natural Key R&D Program of China (Basic Research Project, Grant No. 2017YFB0306104).

## Appendix A. Supplementary data

Supplementary data to this article can be found online at <https://doi.org/10.1016/j.scriptamat.2018.04.022>.

## References

- [1] R.T. Wu, R.C. Reed, *Acta Mater.* 56 (3) (2008) 313–323.
- [2] N.P. Padture, M. Gell, E.H. Jordan, *Science* 296 (5566) (2002) 280–284.
- [3] A. Cipitria, I.O. Golosnoy, T.W. Clyne, *Acta Mater.* 57 (4) (2009) 993–1003.
- [4] E. Bakan, R.J. Vaßen, *Therm. Spray Technol.* 26 (6) (2017) 992–1010.
- [5] R. Darolia, *Int. Mater. Rev.* 58 (2013).
- [6] T.R. Kakuda, A.M. Limarga, T.D. Bennett, D.R. Clarke, *Acta Mater.* 57 (8) (2009) 2583–2591.
- [7] K.V. Niessen, M. Gindrat, A. Refke, *J. Therm. Spray Technol.* 19 (2010) 1–2.
- [8] F. Klaus, C. Ley, *Appl. Ceram. Technol.* 1 (4) (2004) 302–315.
- [9] T.R. Kakuda, A.M. Limarga, T.D. Bennett, D.R. Clarke, *Acta Mater.* 57 (8) (2009) 2583–2591.
- [10] P.L. Fauchais, J.V.R. Heberlein, M.I. Boulos, *Thermal Spray Fundamentals*, Springer Science+Business Media, New York, 2014.
- [11] J. Feng, X. Ren, X. Wang, R. Zhou, W. Pan, *Scr. Mater.* 66 (1) (2012) 41–44.
- [12] G. Mauer, R. Vaßen, D. Stöver, *Surf. Coat. Technol.* 201 (2008) 4374–4381.
- [13] O.P. Solonenko, M.F. Zhukov (Eds.), *Thermal Plasma and New Materials Technology Vol.1 Investigation and Design of Thermal Plasma Generators*, Cambridge Interscience Publishing 1994, pp. 5–43.
- [14] E. Noguees, M. Vardelle, P. Fauchais, P. Granger, *Surf. Coat. Technol.* 202 (18) (2008) 4387–4393.
- [15] K. Von Niessen, M. Gindrat, J. Refke, *Therm. Spray Technol.* 19 (1–2) (2010) 502–509.
- [16] P.J. Phys.D. Fauchais, *Appl. Phys.* 37 (9) (2004) R86–R108.
- [17] P. Fauchais, M. Vardelle, A. Vardelle, S.J. Goutier, *Therm. Spray Technol.* 24 (7) (2015) 1120–1129.
- [18] B. Bernard, A. Quet, L. Bianchi, A. Joulia, A. Malié, V. Schick, B. Rémy, *Surf. Coat. Technol.* 318 (2017) 122–128.
- [19] F. Cernuschi, L. Lorenzoni, S. Capelli, C. Guardamagna, M. Karger, R. Vaßen, C. Giolli, *Wear* 271 (11–12) (2011) 2909–2918.
- [20] G. Mauer, A. Hospach, R. Vaßen, *Surf. Coat. Technol.* 220 (2013) 219–224.
- [21] C. Li, H. Guo, L. Gao, L. Wei, S. Gong, H.J. Xu, *Therm. Spray Technol.* 24 (3) (2014) 534–541.
- [22] Sen Hui Liu, Chen Xin Li, A.B. Murphy, Chang Jiu Li, *Plasma Chem. Plasma Process.* (2017) under review.
- [23] [https://www.oerlikon.com/ecomaXL/files/oerlikon\\_DSMTS0019.2\\_8YO\\_ZrO\\_Agglom.pdf&download=1](https://www.oerlikon.com/ecomaXL/files/oerlikon_DSMTS0019.2_8YO_ZrO_Agglom.pdf&download=1).
- [24] Sen Hui Liu, Chen Xin Li, Chang Jiu Li, et al., *Surf. Coat. Technol.* 337 (2018) 241–249.
- [25] B. Cheng, Y.-M. Zhang, N. Yang, et al., *J. Am. Ceram. Soc.* 100 (2017) 1820–1830.
- [26] <http://www.astm.org/DATABASE.CART/HISTORICAL/E1461-07.htm> 2007.
- [27] L. Vincenzi, S. Suzuki, D. Outcalt, J.J. Heberlein, *Therm. Spray Technol.* 19 (June) (2010) 713–722.
- [28] C. Zhang, W. Li, M. Planche, C. Li, H. Liao, *Surf. Coat. Technol.* 202 (2008) 5055–5061.
- [29] V. Debout, A. Vardelle, P. Fauchais, E. Meillot, E. Bruneton, F. Enguehard, S. Schelz, *High Temp. Mater. Process* 11 (2007) 309–320.
- [30] G. Mauer, R. Vaßen, D. Stöver, *Surf. Coat. Technol.* 204 (1–2) (2009) 172–179.
- [31] A. Refke, G. Barbezat, *Inter. Therm. Spray Confer.* 2003 (May) (2003) 581–588.
- [32] <http://www.tecnar.com/dpv-evolution/>.
- [33] Ashish Ganvir, Nicholas Curry, Nicolaie Markocsan, P. Nylén, Shrikant Joshi, Monika Vilemova, Z. Pala, *Therm. Spray Technol* 25 (January) (2016) 202–212.